Structural Engineering and Mechanics, Vol. 4, No. 1 (1996) 49-59
DOI: http://dx.doi.org/10.12989/sem.1996.4.1.049

Large deflection of simple variable-arc-length beam subjected to a point load

S. Chucheepsakul† and G. Thepphitak‡
Department of Civil Engineering, King Mongkut's Institute of Technology Thonburi, Bangkok 10140, Thailand

C.M. Wang‡†
Department of Civil Engineering, The National University of Singapore, Kent Ridge 0511, Singapore

Abstract. This paper considers large deflection problem of a simply supported beam with variable arc length subjected to a point load. The beam has one of its ends hinged and at a fixed distance from this end propped by a frictionless support over which the beam can slide freely. This highly nonlinear flexural problem is solved by elliptic-integral method and shooting-optimization technique, thereby providing independent checks on the new solutions. Because the beam can slide freely over the frictionless support, there is a maximum or critical load which the beam can carry and it is dependent on the position of the load. Interestingly, two possible equilibrium configurations can be obtained for a given load magnitude which is less than the critical value. The maximum arc-length was found to be equal to about 2.19 times the fixed distance between the supports and this value is independent of the load position.

Key words: bar; beam; elastica; elliptic-integrals; shooting-optimization, large deflections; variable-arc-length beam

1. Introduction

Most research studies on large deflection of beams dealt with beams of given constant deformed arc-length. They are reported in, for examples, Frisch-Fay (1962), Wang (1968), Prathap and Varadan (1975), Theocaris and Panayotounakos (1982), and Fertis and Afonta (1990). In contrast, there has been relatively few studies made on the bending problem of variable deformed arc-length beams. Conway (1947) and Gospodnetic (1959) presented closed-form solutions for such variable-arc-length beams under a central point load. Schile and Sierakowski (1967) gave solutions for this kind of beam under two point loads. More recently, Chucheepsakul (1994, 1995) tackled the large deflections of variable-arc-length beams under moment gradient. The variableness of the deformed arc-length may arise from considering one end of the beam being hinged and allowing the beam to slide freely on a frictionless support located at a specified distance away from this hinged end. In view to obtain independent verification of the bending solutions, Chucheepsakul *et al.* solved the problem using three different approaches, *viz.*

(1) the elliptic-integral method,
(2) the shooting-optimization method and

† Associate Professor
‡ Graduate Student
‡† Senior Lecturer

(3) the finite element method.

This kind of beam bending problem finds application in offshore engineering and deep ocean mining operations. In such applications, the beam may be considered as a link between a spot on the seafloor and the specified location at the seasurface. Owing to the beam undergoing large displacements, the total arc-length of beam is not known and must be determined. In a real condition, the loading is very complex. However, as a first step in understanding the behavior of this class of beam, this paper considers the beam under a single point load. Unlike earlier studies by Conway and by Gospodnetic, the point load is not restricted to a central location between the supports.

The foregoing large deflection problem is solved using the elliptic-integral method and the shooting-optimization method (Wang and Kitipornchai 1992). Interesting features of this problem such as the possibility of having two equilibrium states for a given load magnitude, the existence of a maximum load (or critical load) and a maximum arc-length for equilibrium are also highlighted.

2. Elliptic-integral formulation

Consider an elastic beam as shown in Fig. 1. It is hinged at and A while supported on a frictionless support at B, a fixed distance L away. On this beam, a point load P is applied vertically at the position βL away from end A. The end rotations at A and B are denoted by θ_A and θ_B and the slope at point load is θ_P.

Fig. 2 shows the free body diagrams of the two segments of the deflected beam. One refers to the portion where $0 \leq x \leq \beta L$ and the other refers to $\beta L \leq x \leq L$. From statical consideration, the bending moment M, of the two parts of the beam is given by

$$M = \begin{cases} P(1-\beta)x + P\beta \tan\theta_B y, & 0 \leq x \leq \beta L \quad (1a) \\ P\beta(L-x) + P\beta \tan\theta_B y, & \beta L \leq x \leq L \quad (1b) \end{cases}$$

where x, y are the Cartesian coordinates with the origin at end A.

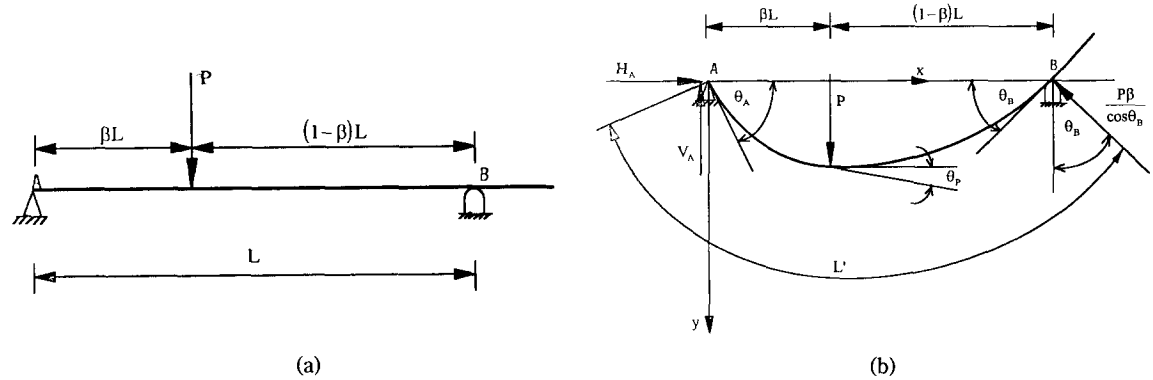

Fig. 1 Elastic beam under a point load: (a) undeflected shape and (b) deflected shape

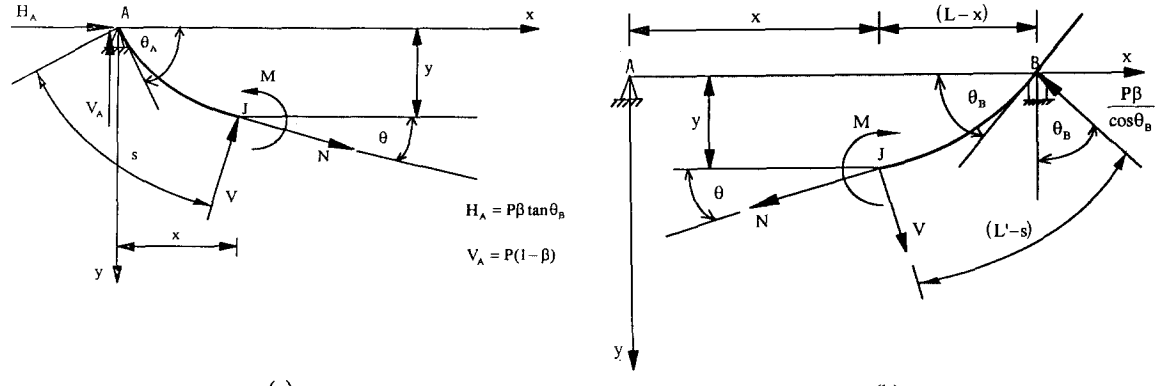

Fig. 2 Free body of two segments of beam

The constitutive relation and the geometric relations are given by

$$M=-EI\frac{d\theta}{ds};\quad \frac{dx}{ds}=\cos\theta,\ \text{and}\ \frac{dy}{ds}=\sin\theta \tag{2a, b, c}$$

In view of Eqs. (2), the equilibrium Eq. (1) after some algebraic manipulations may be written as

$$\frac{EI}{2}\left(\frac{d\theta}{ds}\right)^2=\begin{cases} -P(1-\beta)\sin\theta+P\beta\tan\beta_B\cos\theta+C_1 & \text{for}\quad \theta_p\le\theta\le\theta_A \quad (3a)\\ P\beta\sin\theta+P\beta\tan\theta_B\cos\theta+C_2 & \text{for}\quad -\theta_B\le\theta\le\theta_p \quad (3b)\end{cases}$$

where C_1 and C_2 are the constants of integration. Applying the boundary condition at end A where $\theta=\theta_A$ and $\frac{d\theta}{ds}=0$ gives

$$C_1=P(1-\beta)\sin\theta_A-P\beta\tan\theta_B\cos\theta_A \tag{4}$$

Upon applying the boundary condition at end B where $\theta=-\theta_B$ and $\frac{d\theta}{ds}=0$, one gets $C_2=0$. At the point of load application, $\theta=\theta_p$ and $\left(\frac{d\theta}{ds}\right)$ in Eqs. (3a) and (3b) are equal. As a result, the following relation can be obtained

$$C_1=P\sin\theta_p+C_2=P\sin\theta_p \tag{5}$$

Eqs. (4) and (5) give the relation of θ_A, θ_B and θ_P as follows;

$$\sin\theta_p-(1-\beta)\sin\theta_A-\beta\tan\theta_B\cos\theta_A=0 \tag{6}$$

The substitution of C_1 and C_2 into Eqs. (3) yields the curvature expression of the beam

$$\frac{d\theta}{ds}=\begin{cases} -\frac{1}{L\lambda}\sqrt{\mu_1+\mu_2\sin\theta+\mu_3\cos\theta} & \theta_p\le\theta\le\theta_A \quad (7a)\\ -\frac{1}{L\lambda}\sqrt{\mu_4\sin\theta+\mu_3\cos\theta} & -\theta_B\le\theta\le\theta_P \quad (7b)\end{cases}$$

where

$$\lambda=\frac{1}{\sqrt{2\overline{P}}},\ \overline{P}=\frac{PL^2}{EI},\ \mu_1=\sin\theta_P,\ \mu_2=-(1-\beta),\ \mu_3=\beta\tan\theta_B,\ \mu_4=\beta \tag{8a-f}$$

The negative sign on the right side of Eqs. (7) is chosen because θ decreases as s increases. Considering Eqs. (7), Eq. (2b) and Eq. (2c), one can express ds, dx and dy as functions of θ and $d\theta$. The integration of these functions yield

For $0\le\overline{x}\le\beta$ or $\theta_p\le\theta\le\theta_A$

$$\overline{s}=-\int_{\theta_A}^{\theta}\frac{\lambda}{\sqrt{\mu_1+\mu_2\sin\theta+\mu_3\cos\theta}}d\theta\begin{cases}=\lambda\eta_1\{F(\pi/2,\ k)-F(\Phi_1,\ k)\},\ \text{if}\ \theta\ge\gamma_1 & (9a)\\ =\lambda\eta_1\{F(\pi/2,\ k)+F(\Phi_1,\ k)\},\ \text{if}\ \theta<\gamma_1 & (9b)\end{cases}$$

$$\overline{x}=-\int_{\theta_A}^{\theta}\frac{\lambda\cos\theta}{\sqrt{\mu_1+\mu_2\sin\theta+\mu_3\cos\theta}}d\theta\begin{cases}=\lambda\eta_2[2\{E(\pi/2,\ k)-E(\Phi_1,\ k)\}\\ -\{F(\pi/2,\ k)-F(\Phi_1,\ k)\}-\eta_3 k\cos\Phi_1],\ \text{if}\ \theta\ge\gamma_1 & (10a)\\ =\lambda\eta_2[2\{E(\pi/2,\ k)+E(\Phi_1,\ k)\}\\ -\{F(\pi/2,\ k)+F(\Phi_1,\ k)\}-\eta_3 k\cos\Phi_1],\ \text{if}\ \theta<\gamma_1 & (10b)\end{cases}$$

$$\overline{y}=-\int_{\theta_A}^{\theta}\frac{\lambda\sin\theta}{\sqrt{\mu_1+\mu_2\sin\theta+\mu_3\cos\theta}}d\theta\begin{cases}=\lambda\eta_4[2\{E(\pi/2,\ k)-E(\Phi_1,\ k)\}\\ -\{F(\pi/2,\ k)-F(\Phi_1,\ k)\}-\eta_5 k\cos\Phi_1],\ \text{if}\ \theta\ge\gamma_1 & (11a)\\ =\lambda\eta_2[2\{E(\pi/2,k)+E(\Phi_1,\ k)\}\\ -\{F(\pi/2,\ k)+F(\Phi_1,\ k)\}-\eta_5 k\cos\phi_1],\ \text{if}\ \theta<\gamma_1 & (11b)\end{cases}$$

where E and F are the elliptic-integrals of the first and second kind respectively. The parameters used in Eqs. (9)-(11) are defined as follows:

$$\overline{x}=\frac{x}{L};\ \overline{y}=\frac{y}{L};\ \overline{s}=\frac{s}{L};\ \Phi_1=\sin^{-1}\sqrt{\frac{\sqrt{\mu_2^2+\mu_3^2}-\mu_2\sin\theta-\mu_3\cos\theta}{\mu_1+\sqrt{\mu_2^2+\mu_3^2}}};$$

$$k=\sqrt{\frac{\mu_1+\sqrt{\mu_2^2+\mu_3^2}}{2\sqrt{\mu_2^2+\mu_3^2}}};\ \gamma_1=\sin^{-1}\frac{\mu_2}{\sqrt{\mu_2^2+\mu_3^2}};\ \eta_1=\frac{\sqrt{2}}{(\mu_2^2+\mu_3^2)^{1/4}};$$

$$\eta_2=\frac{\sqrt{2\mu_3}}{(\mu_2^2+\mu_3^2)^{3/4}};\ \eta_3=\frac{2\mu_2}{\mu_3};\ \eta_4=\frac{\sqrt{2\mu_2}}{(\mu_2^2+\mu_3^2)^{3/4}};\ \eta_5=\frac{2\mu_3}{\mu_2} \tag{12a-k}$$

in which μ_1, μ_2 and μ_3 are given in Eqs. (8c)-(8e).

For $\beta\le\overline{x}\le1$ or $-\theta_B\le\theta\le\theta_P$

$$\overline{s}=-\int_{u}^{-\theta_B}\frac{\lambda}{\sqrt{\mu_4\sin\theta+\mu_3\cos\theta}}d\theta\begin{cases}=\lambda\eta_6\{F(\Phi_2,\ 1\sqrt{2})-F(\pi/2,\ 1/\sqrt{2})\},\ \text{if}\ \theta\le\gamma_2 & (13a)\\ =\lambda\eta_6\{F(\Phi_2,\ 1\sqrt{2})+F(\pi/2,\ 1/\sqrt{2})\},\ \text{if}\ \theta>\gamma_2 & (13b)\end{cases}$$

$$\overline{x}=-\int_{\theta}^{-\theta_B}\frac{\lambda\cos\theta}{\sqrt{\mu_4\sin\theta+\mu_3\cos\theta}}d\theta\begin{cases}=\lambda\eta_7[\{F(\Phi_2,\ 1/\sqrt{2})-F(\pi/2,\ 1/\sqrt{2})\}\\ -2\{E(\Phi_2,\ 1/\sqrt{2})-E(\pi/2,\ 1/\sqrt{2})\}+\eta_8\cos\Phi_2],\ \text{if}\ \theta\le\gamma_2 & (14a)\\ =\lambda\eta_7[2\{E(\Phi_2,\ 1/\sqrt{2})+E(\pi/2,\ 1/\sqrt{2})\}\\ -\{F(\Phi_2,\ 1/\sqrt{2})+F(\pi/2,\ 1/\sqrt{2})\}+\eta_8\cos\Phi_2],\ \text{if}\ \theta>\gamma_2 & (14b)\end{cases}$$

$$\overline{y}=-\int_{u}^{-\theta_B}\frac{\lambda\sin\theta}{\sqrt{\mu_4\sin\theta+\mu_3\cos\theta}}d\theta\begin{cases}=\lambda\eta_9[\{F(\Phi_2,\ 1/\sqrt{2})-F(\pi/2,\ 1/\sqrt{2})\}\\ -2\{E(\Phi_2,\ 1/\sqrt{2})-E(\pi/2,\ 1/\sqrt{2})\}-\eta_{10}\cos\Phi_2],\ \text{if}\ \theta\le\gamma_2 & (15a)\\ =\lambda\eta_9[2\{E(\Phi_2,\ 1/\sqrt{2})+E(\pi/2,\ 1/\sqrt{2})\}\\ -\{F(\Phi_2,\ 1/\sqrt{2})+F(\pi/2,\ 1/\sqrt{2})\}-\eta_{10}\cos\Phi_2],\ \text{if}\ \theta>\gamma_2 & (15b)\end{cases}$$

where

$$\Phi_2=\sin^{-1}\sqrt{\frac{\sqrt{\mu_4^2+\mu_3^2}-\mu_4\sin\theta-\mu_3\cos\theta}{\sqrt{\mu_4^2+\mu_3^2}}};\quad \gamma_2=\sin^{-1}\frac{\mu_4}{\sqrt{\mu_4^2+\mu_3^2}};$$

$$\eta_6=\frac{-\sqrt{2}}{(\mu_4^2+\mu_3^2)^{1/4}};\quad \eta_7=\frac{\sqrt{2\mu_3}}{(\mu_4^2+\mu_3^2)^{3/4}}\quad \eta_8=\frac{\sqrt{2\mu_4}}{\mu_3};\quad \eta_9=\frac{\sqrt{2\mu_4}}{\sqrt{(\mu_4^2+\mu_3^2)^{3/4}}}$$

$$\eta_{10}=\frac{\sqrt{2\mu_3}}{\mu_4} \tag{16a-g}$$

in which μ_3 and μ_4 are given in Eqs. (8e)-(8f).

In view of the foregoing elliptic-integral formulation, for a given value of $\bar{P}$ there are three unknowns to be evaluated, *viz.* θ_A, θ_B and θ_P for solution and thus three equations are needed. The first equation is obtained by setting $\bar{x}=\beta$ and $\theta=\theta_P$ in Eq. (10). This result is

$$-\int_{\theta_A}^{-\theta_P}\frac{\lambda\cos\theta}{\sqrt{\mu_1+\mu_2\sin\theta+\theta_3\cos\theta}}d\theta=\beta \tag{17a}$$

The second equation is obtained by setting $\bar{x}=1-\beta$ and $\theta=\theta_P$ in Eq. (14), thus

$$-\int_{\theta_\Pi}^{-\theta_B}\frac{\lambda\cos\theta}{\sqrt{\mu_4\sin\theta+\mu_3\cos\theta}}d\theta=1-\beta \tag{17b}$$

The third equation is given in Eq. (6).

As the foregoing three Eqs. (6), (17a) and (17b) are nonlinear, the solution θ_A, θ_B and θ_P for a given value of $\bar{P}$ have to be obtained by an iterative procedure. The procedure is terminated when the obtained results satisfy the specified tolerance. In many cases, there are some difficulties in obtaining the solutions by the aforementioned procedure. At a specific location of the point load, if the assigned value of $\bar{P}$ is greater than the maximum or critical load $\bar{P}_{cr}$ (see definition below), of that location, the iterative procedure will not converge. An alternative procedure is hence recommended. In this procedure, instead of solving for three unknowns, only two unknowns θ_A or θ_B and θ_P are to be solved. By combining Eqs. (17a) and (17b), so that they are replaced by

$$(1-\beta)\int_{\theta_A}^{\theta_P}\frac{\cos\theta}{\sqrt{\mu_1+\mu_2\sin\theta+\mu_3\cos\theta}}d\theta-\beta\int_{\theta_P}^{-\theta_B}\frac{\cos\theta}{\sqrt{\mu_4\sin\theta+\mu_3\cos\theta}}d\theta=0 \tag{18}$$

The integral terms in Eq. (18) are then replaced by elliptic-integral expressions as given in Eqs. (10a), (10b), (14a) and (14b). Eqs. (6) and (18) are used to solve the problem. The solution steps are as follows:

(1) Assign the value of θ_A, $0\le\theta_A\le\pi/2$, if $\beta\le0.5$ or assign the value of θ_B, $0\le\theta_B\le\pi/2$, if $\beta>0.5$.

(2) Solve for θ_A (or θ_B) and θ_P in Eqs. (6) and (18) by the Newton-Raphson iterative procedure based on the value of θ_A (or θ_B) given in Step 1.

(3) Evaluate Eq. (17a) or Eq. (17b) to obtain $\bar{P}$ for the values of θ_A (or θ_B) and θ_P obtained from Step 2.

(4) Add an increment $\Delta\theta_A$ (or $\Delta\theta_B$) to θ_A (or θ_B) to get the new values of θ_A (or θ_B).

(5) Repeat Steps 2-5 and construct the curves of $\bar{P}$ versus θ_A and θ_B with different values of θ_A or θ_B assigned.

3. Shooting-optimization method

In order to check the validity of the foregoing elliptic-integral formulation and results, the shooting-optimization method (Wang and Kitipornchai 1992) is used to solve the same problem.

In view of Eqs. (1) and (2), the governing differential equations and the boundary conditions can be written as

$$\frac{d\theta}{ds^*} = \overline{PL}[\langle \bar{x}-\beta \rangle - (1-\beta)\bar{x} - \beta\bar{y}\tan\theta_B]; \quad \theta(0)=\theta_A; \quad \theta(1)=-\theta_B \tag{19a,b,c}$$

$$\frac{d\bar{x}}{ds^*} = \bar{L}\cos\theta; \quad \bar{x}(0)=0; \quad \bar{x}(1)=1 \tag{20a,b,c}$$

$$\frac{d\bar{y}}{ds^*} = \bar{L}\sin\theta; \quad \bar{y}(0)=0; \quad \bar{y}(1)=0 \tag{21a,b,c}$$

where

$$s^*=\frac{s}{L}; \quad \bar{L}=\frac{L'}{L} \tag{22}$$

The singularity function $\langle x-\beta L \rangle$ in Eq. (19a), identified by the angle brackets, is defined to be zero if $(x-\beta L)$ is negative and is equal to $(x-\beta L)$ if $(x-\beta L)$ is positive. It is the product of a Heaviside step function with the straight line function $(x-\beta L)$.

The three first-order differential equations contain four unknowns (θ, $\bar{x}$, $\bar{y}$, and $\bar{L}$). There are four given end conditions ($\bar{x}(0)$, $\bar{x}(1)$, $\bar{y}(0)$, and $\bar{y}(1)$) Thus, the unknowns may be solved as functions of $\bar{s}$.

In the solution procedure, the set of differential equations is integrated forward using the fourth-order Runge-Kutta algorithm. The sum Φ of the L_1 error norms given by the differences in values of θ, $\bar{x}$, $\bar{y}$ between the prescribed and the computed terminal boundary conditions is minimized by any standard direct search optimization technique. The objective function of the optimization is given by

$$\begin{aligned} &\text{Minimize} \quad \Phi = |\theta(1)+\theta_B| + |\bar{x}(1)-1| + |\bar{y}(1)| \\ &\theta_A,\ \theta_B,\ \bar{L} \end{aligned} \tag{23}$$

In the computation, the desired value of Φ is that of zero for solution. The simplex method

Table 1 Comparison between results obtained from EIM and SOM for $\bar{P}=6$

β	θ_A(rad)				θ_B(rad)				$\bar{L}$			
	Stable		Unstable		Stable		Unstable		Stable		Unstable	
	EIM	SOM	EIM	SOM	EIM	SOM	EIM	SOM	EIM	SOM	EIM	SOM
0.25	0.3453	0.3452	1.2991	1.2991	0.2496	0.2496	1.1634	1.1635	1.0221	1.0221	1.5593	1.5593
0.50	0.4708	0.4708	0.8760	0.8760	0.4708	0.4708	0.8760	0.8760	1.0617	1.0617	1.2391	1.2391
0.75	0.3126	0.3126	0.6804	0.6804	0.4134	0.4134	0.8012	0.8013	1.0333	1.0333	1.1534	1.1534

EIM = Elliptic-Integral Method
SOM = Shooting-Optimization Method

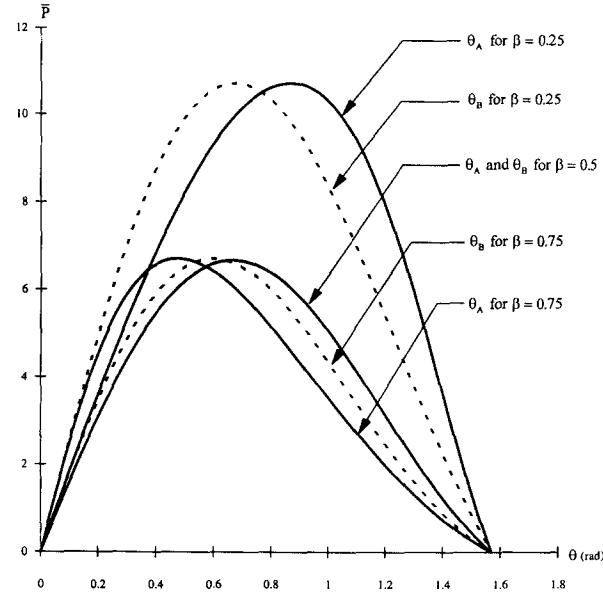

Fig. 3 Variation of the load parameter, $\overline{P}$ with respect to the slope θ_A and θ_B

Table 2 $\overline{P}_{cr}$ for various values of β

β	$\overline{P}_{cr}$
0.05	48.5698
0.15	16.8718
0.25	10.7271
0.35	8.2447
0.45	7.0245
0.50	6.6718
0.55	6.4447
0.65	6.3241
0.75	6.7093
0.85	8.0430
0.95	13.4826

of Nelder and Mead (1964) has been adopted for the optimization algorithm.

4. Comparison of numerical results and comments

As a check on the analytical solutions, results obtained from both the elliptic-integral method and the shooting-optimization method are compared. Table 1 shows a typical comparison of the pertinent values of the end rotations (θ_A and θ_B) and the arc-length $\overline{L}$ for $\overline{P}=6$, $\beta=0.25$, 0.50 and 0.75. As can be seen, the results obtained from the two methods are almost the same; thus confirming the correctness of these new results. Fig. 3 shows the variations of the load $\overline{P}$ with respect to the end slopes θ_A and θ_B and for $\beta=0.25$, 0.50 and 0.75. As can be seen

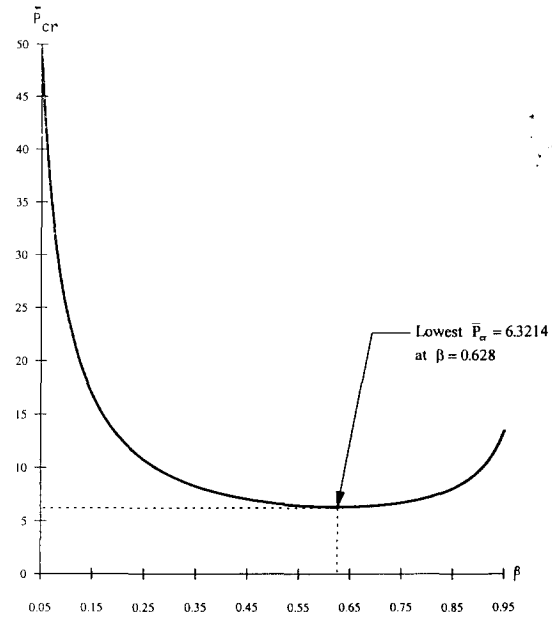

Fig. 4 Plot of $\bar{P}_{cr}$ versus β

from Fig. 3, there is a peak value of $\bar{P}$ for each β. This peak value P_{cr} is referred to as the maximum or critical load at a specific location of the point of application. This value can be determined numerically using Dichotomous search algorithm (Kempf 1987) during the numerical calculation in Step 3. Table 2 shows the numerical values of $\bar{P}_{cr}$ for different values of β. At β=0.5, the $\bar{P}_{cr}$ of 6.6718 is identical to the one given by Gospodnetic (1959) who treated the symmetrical problem of beam sliding freely over both end supports. Fig. 4 shows the plot of $\bar{P}_{cr}$ versus as given in Table 2. It can be seen that there exists a minimum value of $\bar{P}_{cr}$=6.3214 at β=0.628. Once the angles θ_A, θ_B and θ_P have been found, the value of the arc-length $\bar{L}=L'/L$ can be determined from Eqs. (9) and (13), and the deflection $\bar{y}$ at any distance $\bar{x}$ from Eqs. (10), (11), (14), and (15).

Numerical values of $\bar{P}$, θ_B or (θ_A), $\bar{y}_{max}$ and $\bar{L}$ are given in Table 3 for different values of θ_A (or θ_B) assigned and for β=0.25, 0.50, and 0.75. It is worth noting the case where $\theta_A=\theta_B=\pi/2$ and $\bar{P}$=0. The values of $\bar{y}_{max}$ and $\bar{L}_{max}$ in this case are equal to 0.8346 and 2.1884, respectively, and deflection curve is symmetrical about the centerline. Since $\bar{P}$=0, it is independent of load position β. If half of the beam is considered, this configuration is corresponding to a large displaced vertical column subjected to a vertical force at the top end that reaches a horizontal plane. The numerical solution for this case of column problem are given by Timoshenko and Gere (1961). The results of this special case are identical to those obtained by Chucheepsakul *et al.* (1995).

It should be noted that there are two possible equilibrium configurations for the range of end rotations considered here. This is also clearly seen from Fig. 3 that there are two equilibrium configuarations for a given value of $\bar{P}$, except when $\bar{P}$ takes on a maximum value. Fig. 5 shows two deflection curves, the stable and unstable equilibrium configurations, for $\bar{P}$=6 and β=0.25, 0.50 and 0.75.

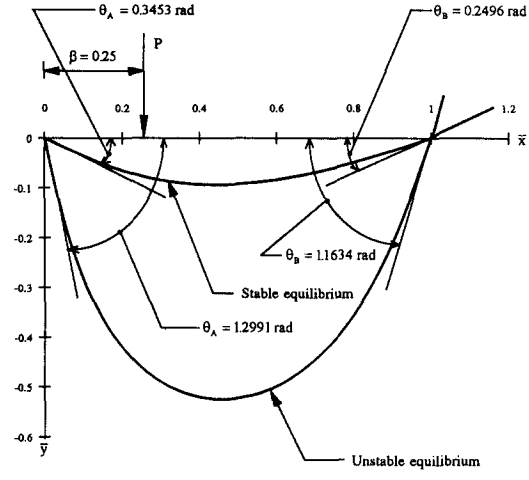

(a)

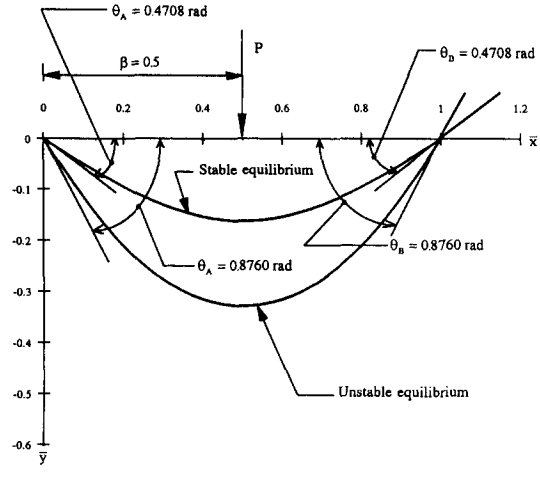

(b)

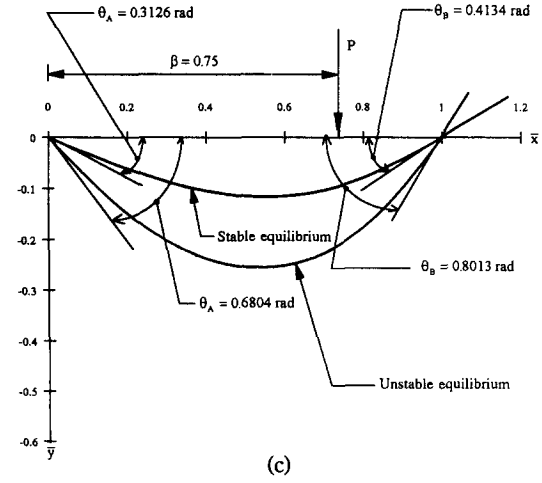

(c)

Fig. 5 Equilibrium configurations for $\bar{P}=6$ and for load at $\beta=0.25$, 0.50, and 0.75

Table 3 Numerical values of θ_A, θ_B, $\overline{P}$, $\overline{y}_{max}$ and $\overline{L}$ for β=0.25, 0.50 and 0.75

β	θ_A		θ_B		$\overline{P}$	$\overline{y}_{max}$	$\overline{L}$
	Degree	Radian	Degree	Radian			
0.25	0	0	0	0	0	0	1.0000
	10	0.1745	7.1642	0.1250	3.1511	0.0467	1.0055
	20	0.3491	14.4631	0.2524	6.0588	0.0949	1.0226
	30	0.5236	22.0497	0.3848	8.4727	0.1465	1.0531
	40	0.6891	30.1232	0.5257	10.1262	0.2039	1.1007
	50	0.8727	38.9639	0.6800	10.7267	0.2708	1.1723
	60	1.0472	48.9804	0.8548	9.9572	0.3535	1.2809
	70	1.2217	60.7386	1.0600	7.5640	0.4631	1.4519
	80	1.3963	74.7177	1.3040	3.7570	0.6176	1.7335
	90	$\pi/2$	90	$\pi/2$	0	0.8346	2.1884
0.50	0	0	0	0	0	0	1.0000
	10	0.1745	10	0.1745	2.7084	0.0584	1.0081
	20	0.3491	20	0.3491	4.9358	0.1184	1.0332
	30	0.5236	30	0.5236	6.3114	0.1816	1.0771
	40	0.6891	40	0.6891	6.6571	0.2503	1.1431
	50	0.8727	50	0.8727	6.0206	0.3270	1.2369
	60	1.0472	60	1.0472	4.6525	0.4158	1.3676
	70	1.2217	70	1.2217	2.9334	0.5225	1.5497
	80	1.3963	80	1.3963	1.2717	0.6565	1.8084
	90	$\pi/2$	90	$\pi/2$	0	0.8346	2.1884
0.75	0	0	0	0	0	0	1.0000
	7.2204	0.1260	10	0.1745	3.0636	0.0468	1.0055
	14.8911	0.2599	20	0.3491	5.4158	0.0962	1.0231
	23.3795	0.4080	30	0.5236	6.5953	0.1507	1.0559
	32.8843	0.5739	40	0.6891	6.5266	0.2132	1.1091
	43.3946	0.7573	50	0.8727	5.4817	0.2896	1.1909
	54.7169	0.9549	60	1.0472	3.9140	0.3764	1.3136
	66.5427	1.1613	70	1.2217	2.2775	0.4885	1.4963
	78.4808	1.3697	80	1.3963	0.9126	0.6349	1.7704
	90	$\pi/2$	90	$\pi/2$	0	.0.8346	2.1884

5. Concluding remarks

Two different methods, the elliptic-integral method and the shooting-optimization method, for solving large deflection of variable-arc-length beam under a point load are presented. The two methods yield almost the same solution. The critical values of $\overline{P}$ can also be obtained in this investigation in which their magnitudes depend on the location of load application. These values correspond to the largest forces which can be applied to the beam at their specific locations. If $\overline{P}<\overline{P}_{cr}$, there are two possible equilibrium configurations. The one with smaller displacement or rotation is stable, while the other is unstable. If $\overline{P}>\overline{P}_{cr}$, no equilibrium state exists. It is also found that the maximum total arc-length is equal to 2.1884 times the fixed distance between the supporting points and this value is independent of the load position β.

References

Chucheepsakul, S., Buncharoen, S., and Wang, C.M. (1994), "Large deflection of beams under moment

gradient," *J. Engrg. Mech., ASCE,* **120**(9), 1848-1860.
Chucheepsakul, S., Buncharoen, S., and Huang, T. (1995), "Elastica of simple variable-arc-length beam subjected to end moment," *J. Engrg. Mech., ASCE,* **121**(7), 767-772.
Conway, H. D. (1947), "The large deflection of a simply supported beam," *Phil. Mag., Series* **7**, 38, 905-911.
Fertis, D. G. and Afonta, A. (1990), "Large deflection of determinate and indeterminate bars of variable stiffness," *J. Engrg. Mech., ASCE,* **116**(7), 1543-1559.
Frisch-Fay, R. (1962), Flexible bars, Butterworths, London, England.
Gospodnetic, D. (1959), "Deflection curve of a simply supported beam," *J. Appl. Mech.,* **26**(4), 675-676.
Kempf, J. (1987), *Numerical software tools in C*, Prentice-Hall, Inc., Englewood Cliffs, New Jersey, NJ., 178-180.
Nelder, J. A. and Mead, R. (1964), "A simplex method for function minimization," *Comp. J.,* 7, 308-313.
Prathap, G. and Varadan, T. K. (1975), "Large deformation of simply supported beam," *J. Engrg. Mech. Div., ASCE,* **101** (EM6), 929-931.
Schile, R. D. and Sierakowski, R. L. (1967), "Large deflection of a beam loaded and supported at two points," *Int. J. Non-linear Mech.* **2**, 61-68.
Theocaris, P. S. and Panayotounakos, D. E. (1982), "Exact solution of the nonlinear differential equation concerning the elastic line of a straight rod due to terminal loading," *Int. J. Non-linear Mech.* **17**(5/6), 395-402.
Timoshenko, S. P. and Gere, J. M. (1961), Theory of elastic stability, McGraw-Hill Book Co., Inc., New York, N. Y., 79-80.
Wang, C. M. and Kitipornchai, S. (1992), "Shooting-optimization technique for large deflection analysis of structural members," *Engrg. Struct.,* **14**(4), 231-240.
Wang, T. M. (1968), "Nonlinear bending of beam with concentrated loads," *J. of Franklin Institute,* **285**, 386-390.